www.nature.com/aps

Acta Pharmacologica Sinica

ARTICLE

Modulating mitochondrial dynamics attenuates cardiac ischemia-reperfusion injury in prediabetic rats

Chayodom Maneechote[1,2,3], Siripong Palee[1,3], Sasiwan Kerdphoo[1,3], Thidarat Jaiwongkam[1,3], Siriporn C. Chattipakorn[1,3] and Nipon Chattipakorn[1,2,3]

Mitochondria are extraordinarily dynamic organelles that have a variety of morphologies, the status of which are controlled by the opposing processes of fission and fusion. Our recent study shows that inhibition of excessive mitochondrial fission by Drp1 inhibitor (Mdivi-1) leads to a reduction in infarct size and left ventricular (LV) dysfunction following cardiac ischemia-reperfusion (I/R) injury in high fat-fed induced pre-diabetic rats. In the present study, we investigated the cardioprotective effects of a mitochondrial fusion promoter (M1) and a combined treatment (M1 and Mdivi-1) in pre-diabetic rats. Wistar rats were given a high-fat diet for 12 weeks to induce prediabetes. The rats then subjected to 30 min-coronary occlusions followed by reperfusion for 120 min. These rats were intravenously administered M1 (2 mg/kg) or M1 (2 mg/kg) combined with Mdivi-1 (1.2 mg/kg) prior to ischemia, during ischemia or at the onset of reperfusion. We showed that administration of M1 alone or in combination with Mdivi-1 prior to ischemia, during ischemia or at the onset of reperfusion all significantly attenuated cardiac mitochondrial ROS production, membrane depolarization, swelling and dynamic imbalance, leading to reduced arrhythmias and infarct size, resulting in improved LV function in pre-diabetic rats. In conclusion, the promotion of mitochondrial fusion at any time-points during cardiac I/R injury attenuated cardiac mitochondrial dysfunction and dynamic imbalance, leading to decreased infarct size and improved LV function in pre-diabetic rats.

Keywords: cardiac ischemia-reperfusion injury; obesity; prediabetes; mitochondrial dynamics; M1; Mdivi-1

Acta Pharmacologica Sinica (2022) 43:26–38; https://doi.org/10.1038/s41401-021-00626-3

INTRODUCTION

Obesity has become one of the major threats to health around the world [1]. Its prevalence has increased in almost every continent and has certainly increased in all developed countries [2]. Long-term exposure to high-fat diet (HFD)-induced obesity, together with excess weight, is presently the most common risk factor for cardiovascular diseases in individuals with established coronary heart disease (CHD) [3]. CHD, also known as ischemic heart disease, is caused by narrowed coronary arteries resulting in myocardial infarction (MI) [4]. The most effective therapeutic intervention currently for reducing acute myocardial ischemic injury and limiting the size of MI is timely and efficient myocardial reperfusion using either thrombolytic therapy or primary percutaneous coronary intervention (PPCI) [5]. However, the process of myocardial reperfusion can itself induce further cardiomyocyte death, a phenomenon known as myocardial ischemia-reperfusion (I/R) injury [6–8]. It is widely accepted that reactive oxygen species (ROS) and cellular Ca^{2+} accumulation play a critical role in I/R-induced injury, including arrhythmogenesis and cardiac function [9–14]. Excessive ROS accumulation results in cellular oxidative stress, mitochondrial dysfunction, and initiation of cell death by activation of the mitochondrial permeability transition pore (mPTP). Elevated ROS levels can also decrease myocardial Ca^{2+} sensitivity, thereby compromising muscle contractile function [15]. Moreover, a reduction in oxidative phosphorylation and a decrease in ATP synthesis are associated with dysfunction in ionic exchangers, thereby resulting in an accumulation of cytosolic Ca^{2+} [9]. These elevated intracellular Ca^{2+} levels are responsible for irreversible damage to cellular integrity due to the activation of degradation enzymes such as lysozymes and phospholipases. According to a previous report on the effects of long-term HFD-induced prediabetes, mild diastolic dysfunction and cardiac hypertrophy associated with prediabetic conditions are multi-factorial phenomena that are associated with early changes in mitophagy, cardiac lipid accumulation, elevated oxidative stress that primarily originates from subsarcolemmal mitochondria, and particularly mitochondrial dynamics alterations [16]. Modulation of mitochondrial dynamics via inhibition of mitochondrial fission and promotion of mitochondrial fusion has been demonstrated to be an effective therapeutic strategy for preventing lethal myocardial reperfusion injury in lean rats [17–19]. However, knowledge regarding their contributions to addressing obesity in a cardiac I/R model is limited.

Mitochondria are extraordinarily dynamic organelles that have a variety of morphologies, the status of which is controlled by the opposing processes of fission and fusion [20, 21]. Mitochondrial

[1]Cardiac Electrophysiology Research and Training Center, Faculty of Medicine, Chiang Mai University, Chiang Mai 50200, Thailand; [2]Cardiac Electrophysiology Unit, Department of Physiology, Faculty of Medicine, Chiang Mai University, Chiang Mai 50200, Thailand and [3]Center of Excellence in Cardiac Electrophysiology Research, Chiang Mai University, Chiang Mai 50200, Thailand
Correspondence: Nipon Chattipakorn (nchattip@gmail.com)

Received: 8 October 2020 Accepted: 9 February 2021
Published online: 12 March 2021

fusion requires three large GTP-hydrolyzing enzymes, Mitofusin 1 (Mfn1) and Mitofusin 2 (Mfn2), both of which are located on the mitochondrial outer membrane and are required for outer membrane fusion [22]. In contrast, inner membrane fusion is mediated by Optic Atrophy 1 (Opa1) [22]. Mitochondrial fission requires dynamin-related protein 1 (Drp1), a large GTPase that oligomerizes the nucleotide GTP and hence constricts the outer mitochondrial membrane [23]. It has been shown that alterations in mitochondrial dynamics play a key role in the pathophysiological mechanisms of both obesity and cardiac I/R injury [24, 25]. Excessive mitochondrial fission caused by a high degree of ROS [26, 27], intracellular Ca^{2+} [28–30], inflammation [30], and lipid accumulation [30, 31] leads to Drp1 activation and subsequently to myocardial cell death. On the other hand, obesity and cardiac I/R impair mitochondrial fusion, as indicated by reduced levels of Mfn1/2 and Opa1 [17, 27]. Although we have already found that inhibiting Drp1 via Mdivi-1 has cardioprotective effects during cardiac I/R injury in prediabetic rats [32], the beneficial effects of the mitochondrial fusion promoter M1 on cardiac function in prediabetic rats with I/R injury have never been investigated.

The mitochondrial fusion promoter agent M1 has been shown to exert cardioprotective effects in lean rats with cardiac I/R injury [27] and in prediabetic rats [33] by restoring the expression of mitochondrial fusion proteins (e.g., Mfn1/2 and Opa1) and mitochondrial function. M1 treatment also effectively improved mitochondrial dynamics balance and ameliorated diabetic cardiomyopathy in an Opa1-dependent manner [34]. Mdivi-1 is a mitochondrial fission inhibitor agent that has been shown to be beneficial in preserving cardiac function in both lean and prediabetic rats with cardiac I/R injury [18, 32]. Mdivi-1 acts on a mitochondrial fission-related protein (Drp1) to inhibit Drp1-induced excessive mitochondrial fission and fragmentation following I/R injury [17].

In this study, we further investigated the promotion of mitochondrial fusion (M1) or a combination of both M1 and the inhibition of fission (Mdivi-1) in prediabetic rats with cardiac I/R injury. We hypothesized that acute M1 treatment prior to ischemia, during the ischemic period, and at the onset of reperfusion exerts cardioprotective effects with different levels of efficacy in prediabetic rats with cardiac I/R injury. In particular, the combined therapies have higher efficacy than a single M1 treatment.

MATERIALS AND METHODS

Animals and experimental designs

Animal experimentation complied with the ARRIVE guidelines [35] and was carried out in accordance with the National Institutes of Health Guide for the Care and Use of Laboratory Animals (NIH) [36]. The protocols were approved by the Institutional Animal Care and Use Committee of the Faculty of Medicine, Chiang Mai University, Thailand (Permit No. 34/2561), and were performed at the Cardiac Electrophysiology Research and Training Center, Faculty of Medicine, Chiang Mai University, Chiang Mai, Thailand. Briefly, male Wistar rats ($n = 80$, ~220 g, ~7-week old) were obtained from Nomura Siam International Co., Ltd., Thailand, and acclimatized in environmentally controlled conditions (25 ± 0.5 °C, 12-h light/12-h dark cycle) with normal rat chow and water ad libitum. After 1 week, all rats were randomly assigned into two groups, either a normal-diet group (ND, a diet containing 19.77% of energy from fat) or a high-fat diet group (HFD, a diet containing 59.28% of energy from fat) [33, 37]. After being fed these specific diets for 12 weeks, blood samples from the tail vein of rats in the ND ($n = 10$) and HFD ($n = 70$) groups were collected to determine metabolic parameters. Next, all rats in the HFD group were subjected to 30-min left anterior descending (LAD) coronary artery occlusion, followed by reperfusion for 120 min and were divided into groups receiving either vehicle (0.1% DMSO, HFV), M1 (2 mg/kg) or combined treatment (M1 2 mg/kg + Mdivi-1 1.2 mg/kg) via iv injections through the femoral vein. M1 single therapy or combined M1 with Mdivi-1 treatment was given at different times during the cardiac I/R period, including (1) 15 min before ischemia (HFPM1 and HFPCom); (2) during ischemia for 15 min (HFDM1 and HFDCom); and (3) at the onset of reperfusion (HFRM1 and HFRCom). During the I/R protocol, LV function was assessed using a pressure-volume (P-V) loop recording device (Transonic Scisense Inc., London, ON, Canada). A lead II surface electrocardiogram (ECG) was used to determine the arrhythmia score. Finally, the heart was rapidly removed under deep anesthesia for infarct size measurement and cardiac tissue studies. The study protocol is shown in Fig. 1.

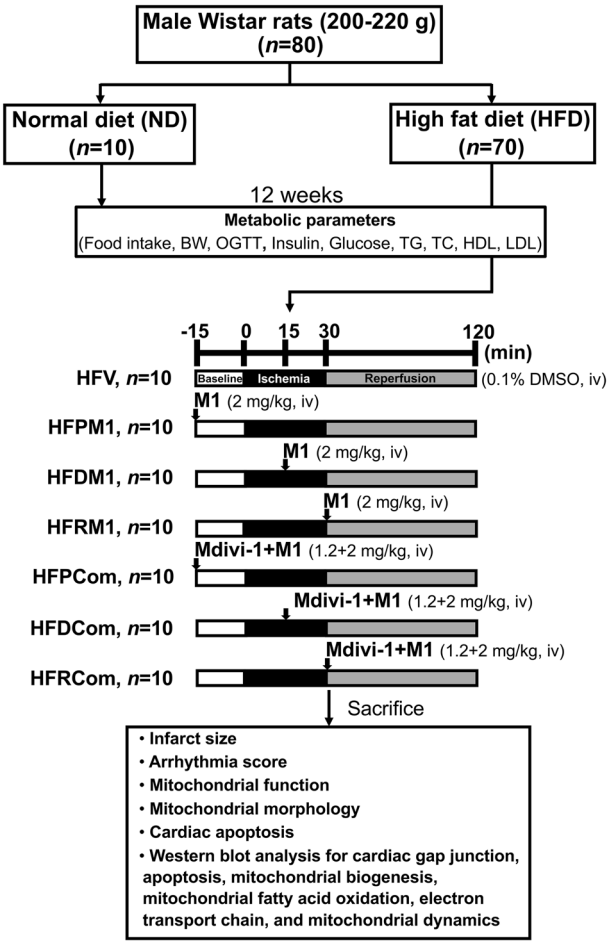

Fig. 1 Diagram of the experimental protocol and dataset for analysis of this study. BW body weight, DMSO dimethyl sulfoxide, HDL high-density lipoprotein, HFD high-fat diet-fed rats, HFDCom high-fat diet-fed rats with Mdivi-1 and M1 treatment during ischemia, HFDM1 high-fat diet-fed rats with M1 treatment during ischemia, HFPCom high-fat diet-fed rats with Mdivi-1 and M1 treatment preischemia, HFPM1 high-fat diet-fed rats with M1 treatment preischemia, HFRCom high-fat diet-fed rats with Mdivi-1 and M1 treatment at the onset of reperfusion, HFRM1 high-fat diet-fed rats with M1 treatment at the onset of reperfusion, HFV high-fat diet-fed rats with vehicle treatment, LDL low-density lipoprotein, ND normal diet-fed rats, OGTT oral glucose tolerance test, TC total cholesterol, TG triglyceride.

Surgical procedure for cardiac I/R injury

Zoletil (50 mg/kg, Vibbac Laboratories, Carros, France) and xylazine (0.15 mg/kg, Laboratorios Calier, S.A., Barcelona, Spain) were used for anesthesia for rats via intramuscular injections. A tracheostomy was performed, and the left femoral vein was

identified and used as the route of drug administration. All rats were heated under a warm pad and ventilated with room air from a positive pressure ventilator (Cwe, Inc., Ardmore, PA, USA). Lead II ECG (PowerLab 4/25T, AD Instrument) was recorded throughout the experiment. Then, a left-side thoracotomy was performed at the fourth intercostal space, and the pericardium was incised. The LAD was identified and ligated ~2 mm distal to its origin with a 5-0 silk suture using a traumatic needle. The end of this ligature was passed through a small vinyl tube, which was used to occlude the LAD by pulling the thread. Ischemia was confirmed by ST-segment elevation on the ECG and a change in the color of the myocardial tissue around the ischemic area. After 30 min of ischemia, the ligature was loosened, and the ischemic myocardium was continuously reperfused for 2 h.

Pressure-volume loop study

A P-V catheter (Transonic Scisense, Ontario, Canada) was inserted into the LV chamber via the right common carotid artery (Rt. CCA). Parameters including the left ventricular ejection fraction (LVEF), left ventricular end-systolic pressure (LVESP) and end-diastolic pressure (LVEDP), maximum and minimum d*p*/d*t* (+d*p*/d*t* and -d*p*/d*t*), stroke volume (SV), and heart rate (HR) were determined using an analytical software program (Labscribe, Dover, New Hampshire, USA) [27]. For P-V loop data analysis, the following steps were taken: (1) 50 loops before ischemia were selected to represent the baseline; (2) 50 loops at the end of coronary occlusion were selected to represent the ischemic period; and (3) 50 loops at the end of reperfusion were selected to represent the reperfusion period.

Arrhythmia score determination

A lead II ECG was used to determine the arrhythmia score as described previously [27]. The occurrence of arrhythmia was characterized using the Lambeth Conventions, and the arrhythmia score was determined based on the criteria of Curtis and Walker.

Myocardial infarct size determination

The heart was perfused with 1 mL of Evan's blue dye through the aorta to determine the LV area at risk (AAR), which is defined as the area that does not turn blue. Then, the heart was frozen at −20 °C overnight and sectioned horizontally from the apex to the occlusion site into 6-7 slices. Next, 2,3,5-triphenyltetrazolium chloride (TTC) (1%) was added to each slice for 15 min at 37 °C. Within the AAR zone, the area with viable tissues was seen in red, whereas the infarct area was seen in white, which was not stained with Evans blue. The infarct size and AAR were determined using ImageJ software version 1.52a and were calculated using a formula as reported previously [27].

Cardiac mitochondrial function study

The rat hearts were removed and perfused with cold 0.9% NSS. The hearts were divided into ischemic (I) and nonischemic or remote (R) areas of the ventricle and chopped into small pieces. Then, cardiac tissues were homogenized and centrifuged according to our previous protocol to isolate cardiac mitochondria. Mitochondrial isolation buffer (MIB) was used to homogenize the cardiac tissue. The MIB was composed of (1) 5 mM TES, sodium salt, (2) 300 mM sucrose, and (3) 0.2 mM EGTA. The pH was adjusted to 7.2 with NaOH and HCl [38, 39]. Briefly, the heart was finely minced and homogenized by a homogenizer in ice-cold MIB buffer. Then, the homogenate was centrifuged at 800 × *g* for 5 min, and the supernatant was collected. The supernatant was then centrifuged at 8800 × *g* for 5 min, and the cytosolic fraction was obtained. Finally, the mitochondrial pellet was again resuspended in ice-cold MIB buffer and centrifuged one more time at 8800 × *g* for 5 min. The mitochondrial fraction was obtained after the third centrifugation [38, 39].

ROS production was measured by adding dichlorodihydrofluorescein diacetate (DCFH-DA) dye and incubating it for 25 min. A fluorescence microplate reader (Gen5 Microplate Reader, BioTek Instruments, VT, USA) with an excitation wavelength of 485 nm and an emission wavelength of 530 nm was used to detect the level of ROS generation from cardiac mitochondria [27].

For mitochondrial membrane potential changes, the 5,5,6,6-tetrachloro-1,1,3,3-tetraethylbenzimidazolcarbocyanine iodide (JC-1) dye was used. The green fluorescence (JC-1 monomer) was excited at a wavelength of 485 nm, and the emission was detected at 590 nm, while the red fluorescence (JC-1 aggregates) was excited at a wavelength of 485 nm, and the emission was detected at 530 nm. A decreased red/green fluorescence intensity ratio indicates depolarization of the mitochondrial membrane [27].

Mitochondrial swelling was determined using spectrophotometry at 25 °C as previously described [27]. Decreased light absorbance in a mitochondrial suspension at 540 nm indicates mitochondrial swelling. In addition, transmission electron microscopy (TEM; JEM-1200 EX II, JEOL Ltd., Japan) was used to determine the morphology of isolated cardiac mitochondria [27].

Determination of cardiac mitochondrial dynamics, biogenesis, apoptosis, and Connexin-43

Western blot analysis was used to determine the protein expression of mitochondrial fission proteins (Drp1 phosphorylated at serine 616 (p-Drp1^{ser616}) in the cytosolic fraction and Drp1 in the mitochondrial fraction), mitochondrial fusion proteins (Mfn1, Mfn2, and Opa1 in the mitochondrial fraction), mitochondrial biogenesis proteins (peroxisome proliferator-activated receptor gamma coactivator 1-alpha (PGC1-α), carnitine palmitoyltransferase I (CPT1), respiratory complexes I-V of the electron transport chain (ETC)), apoptotic proteins (Bax, Bcl-2, cytochrome *c* (Cyt *c*), caspase-3 and cleaved caspase-3), cardiac gap junction proteins (connexin-43 phosphorylated at serine 368 (p-Cx43^{ser368}) and connexin-43 (Cx43)), β-actin, and voltage-dependent anion channel (VDAC) in the heart. Briefly, myocardial protein extracts, cardiac mitochondrial fraction, and cytosolic fraction were divided into ischemic (I) and nonischemic or remote (R) areas. Protein concentrations from the heart tissues and cytosol were determined using a Bio-Rad protein assay kit (Bio-Rad Laboratories, Hercules, CA, USA). Protein (50-80 μg) was added to the loading buffer and mixed with a loading buffer consisting of 5% mercaptoethanol, 0.05% bromophenol blue, 75 nM Tris, 2% SDS, and 10% glycerol at pH 6.8). Then, the mixture was boiled for 5 min and loaded into 10% gradient SDS-polyacrylamide gels. Proteins were then transferred to a nitrocellulose membrane in the presence of glycine/methanol transfer buffer (containing 20 mM Tris, 0.15 M glycine, and 20% methanol) in a transfer system (Bio-Rad). The membranes were incubated in 5% skim milk in 1× TBST buffer (containing 20 mM Tris (pH 7.6), 137 nM NaCl, and 0.05% Tween-20) for 1 h at room temperature and then exposed to anti-Drp1 (1:1000 dilution; rabbit; Cell Signaling #5391), anti-p-Drp1^{Ser616} (1:1000 dilution; rabbit; Cell Signaling #3455), anti-Mfn1 (1:1000 dilution; rabbit; Cell Signaling #13196), anti-Mfn2 (1:1000 dilution; rabbit; Cell Signaling #9482), anti-Opa1 (1:1,000 dilution; rabbit; Cell Signaling #80471), anti-PGC1-α (1:200 dilution; mouse; Santa Cruz sc-518038), anti-CPT1 (1:1000 dilution; mouse; Santa Cruz sc-514555), anti-respiratory complexes I-V (1:1000 dilution; mouse; Santa Cruz sc-518038), anti-Bax (1:1000 dilution; rabbit; Cell Signaling #5023), anti-Bcl-2 (1:1000 dilution; rabbit; Cell Signaling #3498), anti-Cyt *c* (1:500 dilution; rabbit; Cell Signaling #4272), anti-Caspase3 (1:1000 dilution; rabbit; Cell Signaling #14220), anti-Cleaved-caspase3 (1:1000 dilution; rabbit; Cell Signaling #14220), anti-p-Cx43^{ser368} (1:1000 dilution; rabbit; Cell Signaling #3511), anti-Cx43 (1:1000 dilution; rabbit; Cell Signaling #3512), anti-VDAC (1:1000 dilution; rabbit; Cell Signaling #4991) and anti-GAPDH (1:1000 dilution; rabbit; Cell Signaling #12741) for 12 h. Bound antibody was detected by the conjugation of horseradish peroxidase with anti-rabbit IgG. Finally, bands were incubated in enhanced chemiluminescence (ECL) detection

reagents and detected using Bio-Rad ChemiDoc™ Imagers (Bio-Rad, CA, USA). The analysis of protein expression was determined using ImageJ software version 1.52a [27].

TUNEL-positive cells for quantification of cardiomyocyte apoptosis
A terminal deoxynucleotidyl transferase (TdT) dUTP nick-end labeling (TUNEL) assay was used to detect cardiomyocyte apoptosis by using an In Situ Cell Death Detection Kit (Roche, Basel, Switzerland). For in situ labeling, cardiac tissue slices from the ischemic area were placed in 1×PBS for 10 min after dehydration. The samples were covered with 50 µL of Proteinase K solution (1:50) for 30 min followed by 50 µL of Cytonin™ for 120 min. For the positive control, the samples were covered with TACS nuclease 1:50 in TACS nuclease buffer. TUNEL-positive cells were detected with a fluorescence microscope (Nikon, Tokyo, Japan) at λ_{ex} 494 nm and λ_{em} 512 nm. DAPI was detected at λ_{ex} 358 nm and λ_{em} 461 nm. The apoptosis index was calculated as a percentage of the number of TUNEL-positive apoptotic cells over the total number of nucleated cells (DAPI staining) [27].

Determination of metabolic parameters
Plasma was prepared from fasted blood samples and was kept frozen at −80 °C until analysis of glucose, cholesterol (TC), triglyceride (TG), and insulin levels could be completed. Plasma insulin levels were detected using a sandwich ELISA kit (Millipore, MI, USA). Plasma glucose and triglyceride levels were determined by colorimetric assay from a commercially available kit (Biotech, Bangkok, Thailand). Fasting plasma high-density lipoprotein (HDL) and low-density lipoprotein (LDL) were determined using commercially available kits (ERBA diagnostic, Mannheim, Germany) [33].

The degree of insulin resistance was assessed by the HOMA index, which was calculated from fasting plasma insulin and fasting plasma glucose concentrations. For the insulin sensitivity test, the OGTT was performed as previously described [33]. Briefly, rats were fasted for 12 h prior to the test; glucose (2 mg/kg) was delivered to the rats by gavage feeding; blood from the tail tip was collected immediately before glucose feeding and at 15, 30, 60, and 120 min after feeding; blood samples were centrifuged and plasma was collected to determine the plasma glucose level during OGTT, with the level being calculated from the total area under the curve (AUCg).

Data and statistical analysis
The experimental procedures and data analyses were carried out with randomization and blinding. Data are expressed as the mean ± SEM. Data were analyzed using GraphPad Prism 8.2.1 software. One-way ANOVA followed by an LSD post hoc test was used to test the difference between groups. The mortality rate was analyzed using the chi-square test. $P < 0.05$ was considered statistically significant.

RESULTS

Metabolic parameters in obese rats
After 12 weeks of HFD consumption, obese rats had significantly increased body weight, visceral fat, plasma insulin, HOMA index, glucose AUCg, TC, and LDL but decreased HDL levels compared with ND-fed rats (Table 1). However, there were no differences in food intake, plasma glucose, or TC levels between the two groups.

Acute M1 treatment reduced the myocardial infarct size, mortality rate, and arrhythmia in prediabetic rats with cardiac I/R
The cardiac I/R rats that received M1 at three different time points showed a significant reduction in myocardial infarct size (Fig. 2a, b). The percentage reduction was 46%, 38%, and 36% for HFPM1, HFDM1, and HFRM1, respectively, when compared to the HFV group. In addition to the M1 treatment, the combined M1 and Mdivi-1 treatment also shared similar efficacy to the M1 treatment in reducing infarct size (HFPCom [47%], HFDCom [41%], and HFRCom [43%] compared to the HFV group) (Fig. 2a, b). The mortality rate also declined in all treatment groups in comparison to the HFV group (Fig. 2c).

It is commonly known that myocardial infarct size is associated with the prevalence of cardiac arrhythmia. We used the arrhythmia scoring system of 0-5 (where a higher score indicates a higher degree of arrhythmia) for the presentation of ventricular arrhythmia. Interestingly, compared with HFV rats, HF rats treated with M1 at three different periods during cardiac I/R showed a significantly lower cardiac arrhythmia score (Fig. 2d). Cx43, a cardiac gap junction protein that allows intercellular communication, can be related to the incidence of arrhythmia. The expression of p-Cx43^{ser368} per total Cx43 in cardiac tissue also showed a significant increase in all M1 groups compared with the HFV group (Fig. 2e). Again, the combined treatment did not show any increase in efficacy when compared to M1 treatment alone (Fig. 2d, e).

Table 1. The metabolic parameters in pre-diabetic I/R rats.

Metabolic parameters	ND	HFD
Body weight (g)	521.5 ± 22.9	643.8 ± 19.3*
Food intake (g/day)	26.7 ± 1.6	27.2 ± 1.1
Visceral fat (g)	28.4 ± 7.3	60.1 ± 4.6*
Plasma glucose (mg/dL)	98.2 ± 11.3	102.7 ± 18.5
Plasma insulin (ng/mL)	2.2 ± 0.5	6.7 ± 1.0*
HOMA index	15.8 ± 3.6	30.3 ± 3.7*
Plasma glucose AUC (AUCg) (mg/dL × min × 10^4)	2.5 ± 0.7	4.7 ± 0.9*
Plasma total cholesterol (mg/dL)	69.8 ± 3.7	109.1 ± 4.3*
Plasma total triglycerides (mg/dL)	98.2 ± 5.4	107.1 ± 7.2
HDL (mg/dL)	26.4 ± 2.2	16.8 ± 2.9*
LDL (mg/dL)	40.1 ± 5.8	72.7 ± 14.8*

Values are mean ± SEM. *$P < 0.05$ vs ND. $n = 10$ in each group.
AUC area under the curve, *HDL* high-density lipoprotein, *HFD* high-fat-diet fed rats, *HOMA* the homeostatic model assessment, *LDL* low-density lipoprotein, *ND* normal-diet fed rats.

Acute M1 treatment attenuated myocardial cell death in prediabetic rats with cardiac I/R
Apoptosis is another major form of cardiomyocyte death following cardiac I/R. We investigated whether acute M1 treatment could reduce I/R-induced myocardial apoptosis under prediabetic conditions. Our results demonstrated that HF rats treated with M1 exhibited suppressed myocardial apoptosis, as indicated by the decreased expression levels of Bax, Cyt *c*, and cleaved-caspase-3 in comparison with those in HFV rats (Fig. 3a-d). We also used TUNEL assays to detect apoptotic DNA fragmentation in cardiac cells. Similar results were found in the M1-treated groups at all treatment periods, in which the number of TUNEL-positive cells, as shown by the apoptosis index, also decreased compared to that in the HFV group (Fig. 3e). The combined treatment did not show greater efficacy than M1 treatment alone (Fig. 3a-e).

Acute M1 treatment improved cardiac mitochondrial function and the balance of mitochondrial dynamics in prediabetic rats with cardiac I/R
Mitochondrial dynamics has a crucial role in controlling mitochondrial function during cardiac I/R [24]. We found that mitochondrial ROS production, membrane potential depolarization, and swelling were significantly attenuated during all periods of acute M1 treatment compared with the HFV group (Fig. 4a-c).

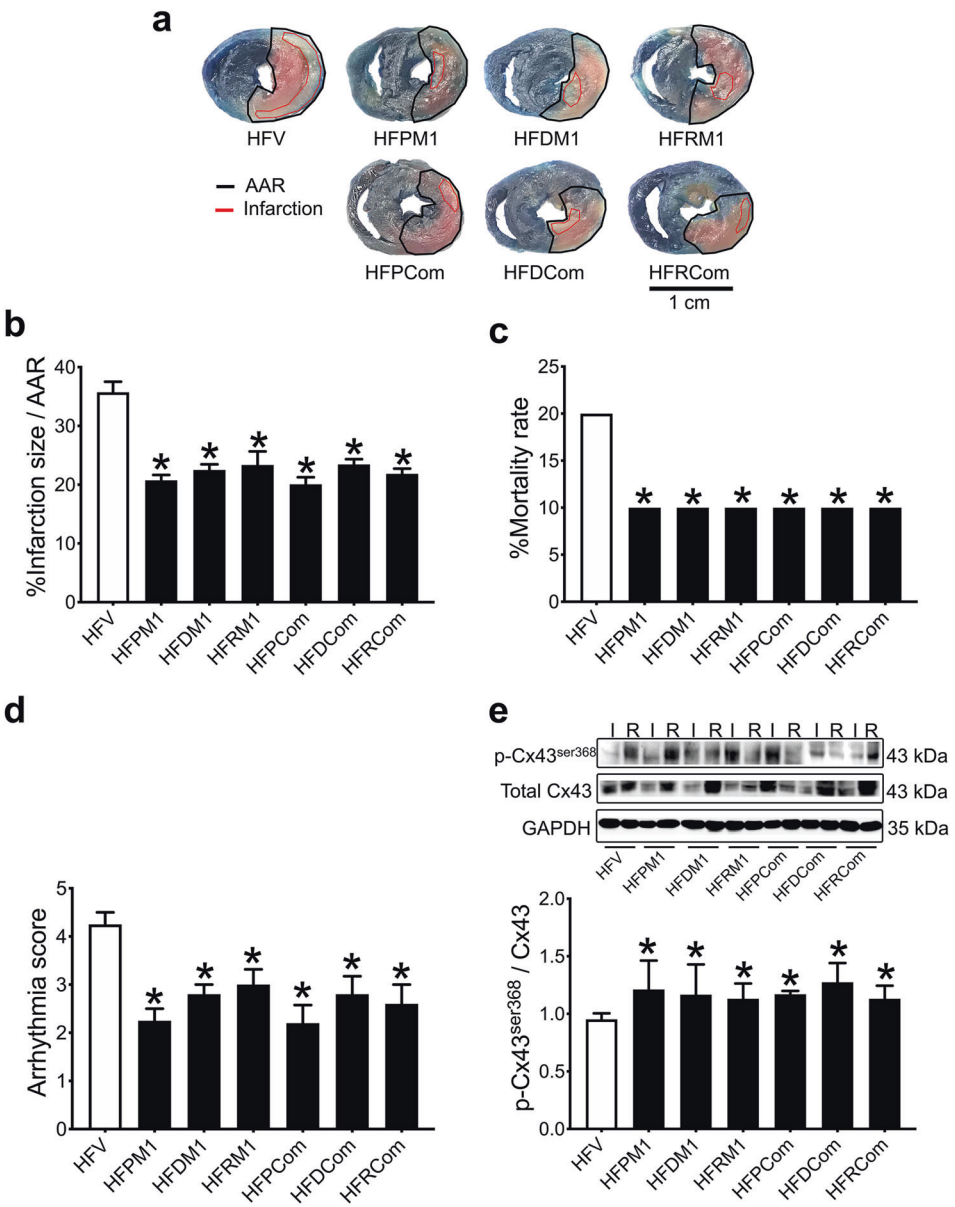

Fig. 2 The effects of acute M1 and combined treatment given at different time points on the myocardial infarct size, mortality rate, cardiac arrhythmia, and cardiac conductivity-related proteins in prediabetic rats with cardiac I/R injury. a Representative images of rat heart slices stained with triphenyl tetrazolium chloride (TTC). **b** %Infarction size per AAR; blue area = perfused and alive; red and white areas = AAR; white area = infarction; scale bar: 1 cm; $n = 5$ per group. **c** Mortality rate; $n = 10$ per group. **d** Arrhythmia score; $n = 5$ per group. **e** p-Cx43^{Ser368} per total Cx43 expression in the ischemic area normalized to that in the remote area; $n = 5$ per group. *$P < 0.05$ vs HFV. AAR area at risk, Cx43 connexin 43, GAPDH glyceraldehyde 3-phosphate dehydrogenase, HFDCom high-fat diet-fed rats with Mdivi-1 and M1 treatment during ischemia, HFDM1 high-fat diet-fed rats with M1 treatment during ischemia, HFPCom high-fat diet-fed rats with Mdivi-1 and M1 treatment preischemia, HFPM1 high-fat diet-fed rats with M1 treatment preischemia, HFRCom high-fat diet-fed rats with Mdivi-1 and M1 treatment at the onset of reperfusion, HFRM1 high-fat diet-fed rats with M1 treatment at the onset of reperfusion, HFV high-fat diet-fed rats with vehicle treatment, p-Cx43^{Ser368} phosphorylation of connexin 43 at serine 368.

Representative TEM images of cardiac mitochondrial morphology revealed the unfolding of cristae and swelling in the ischemic tissue of HFV rats (Fig. 4d). The swelling in these mitochondria was markedly decreased after treatment with M1 at any time in relation to cardiac I/R. The combined treatment did not show any greater efficacy than M1 treatment alone (Fig. 4a-d).

It has been suggested that, as one major regulator of mitochondrial fission, Drp1 typically resides in an inactive form in the cytosol and upon activation is translocated into the mitochondria following cardiac I/R injury and in obese conditions. Our results showed that the protein expression of activated Drp1 (p-Drp1^{ser616}) in the cytosol and total Drp1 in the mitochondrial fraction was decreased in the combined treatment group but not in the M1 treatment group compared to the HFV group (Fig. 4e, f). In addition, three mitochondrial fusion proteins (Mfn1, Mfn2, and Opa1) exhibited increased expression levels after treatment with M1 compared to the HFV group (Fig. 4g-h). The combined treatment did not show any increase in efficacy in comparison to the M1 treatment alone.

Acute M1 treatment increased cardiac mitochondrial biogenesis and metabolism in prediabetic rats with cardiac I/R

To determine whether an alteration in mitochondrial dynamics was associated with mitochondrial function in prediabetic rats

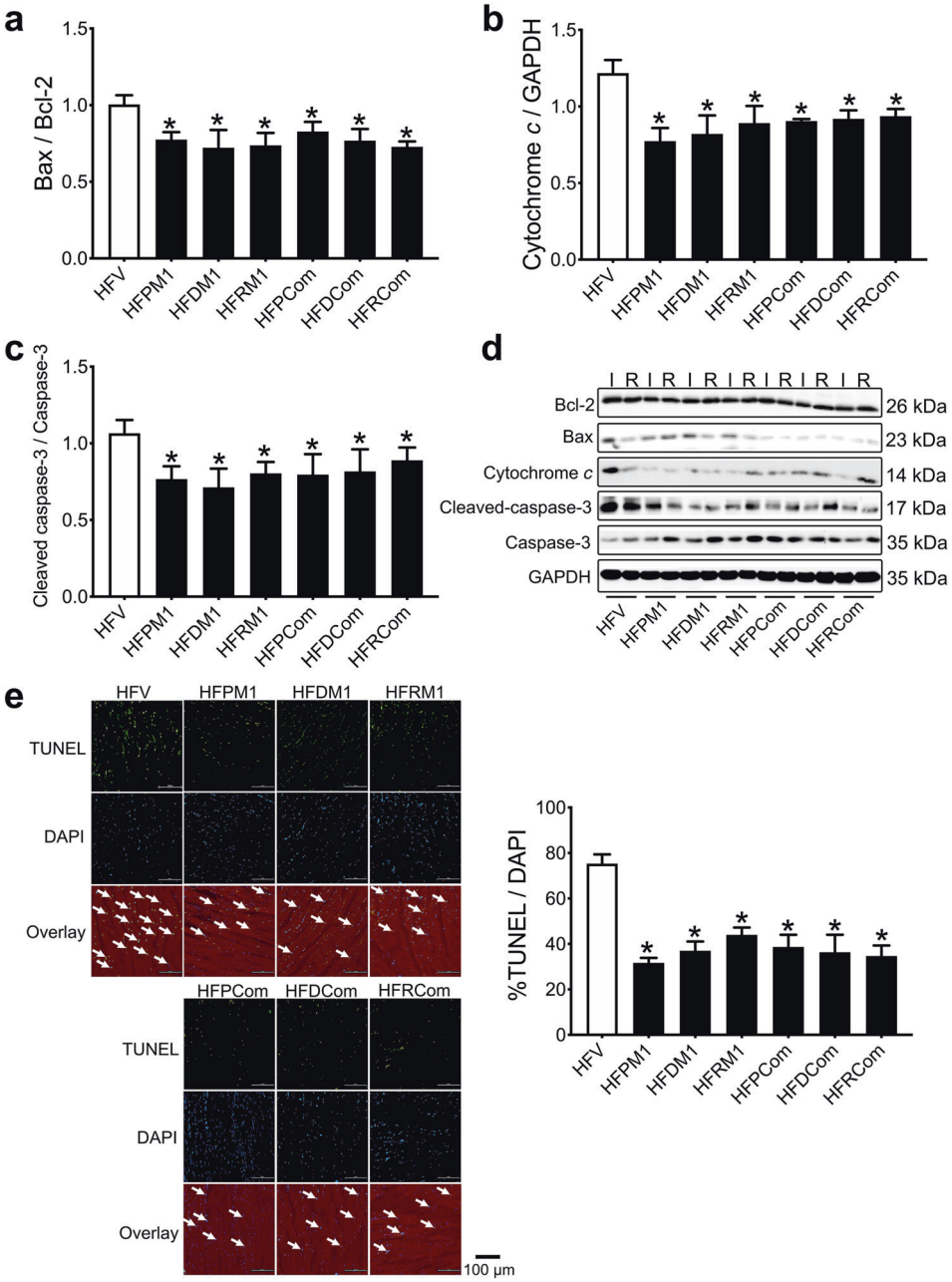

Fig. 3 The effects of acute M1 and combined treatment at different time points on apoptotic proteins and TUNEL-positive cells in prediabetic rats with cardiac I/R injury. a Bax per Bcl-2 expression; **b** Cytochrome *c* expression; **c** Cleaved caspase-3 per total caspase-3 expression; **d** Representative images of Western blotting bands; **e** TUNEL-positive cells (scale bar = 100 μm) in the ischemic area normalized to that in the remote area. $n = 5$ per group. $^*P < 0.05$ vs HFV. Bax Bcl2-associated X protein, Bcl-2 B-cell lymphoma 2, DAPI 4′,6-diamidino-2-phenylindole, GAPDH glyceraldehyde 3-phosphate dehydrogenase, HFDCom high-fat diet-fed rats with Mdivi-1 and M1 treatment during ischemia, HFDM1 high-fat diet-fed rats with M1 treatment during ischemia, HFPCom high-fat diet-fed rats with Mdivi-1 and M1 treatment preischemia, HFPM1 high-fat diet-fed rats with M1 treatment preischemia, HFRCom high-fat diet-fed rats with Mdivi-1 and M1 treatment at the onset of reperfusion, HFRM1 high-fat diet-fed rats with M1 treatment at the onset of reperfusion, HFV high-fat diet-fed rats with vehicle treatment, TUNEL terminal deoxynucleotidyl transferase dUTP nick end labeling.

with cardiac I/R, we measured the expression of PGC1-α (mitochondrial biogenesis), CPT1 (fat metabolism) and mitochondrial complex I/II/III/IV/V (oxidative phosphorylation) levels using Western blotting. Here, we found that only the PGC1-α level was significantly increased in all M1 treatment groups compared with the HFV group (Fig. 5a, h). In contrast, there were no differences in CPT1 and mitochondrial complex I-V levels between the HFV and all treated groups (Fig. 5b-h). The combined treatment did not show any greater efficacy than M1 treatment alone.

Acute M1 treatment improved cardiac function in prediabetic rats with cardiac I/R

Evaluation of the pressure-volume loop analysis during cardiac I/R revealed that SV, LVESP, +d*p*/d*t* and LVEF were markedly decreased, while LVEDP and -d*p*/d*t* were increased in all groups during the ischemic period (Fig. 6b, c, e, f, and g) compared with their respective baseline periods. However, at the end point of reperfusion, M1 treatment at three different time points resulted in an improvement in all of those hemodynamic measurements

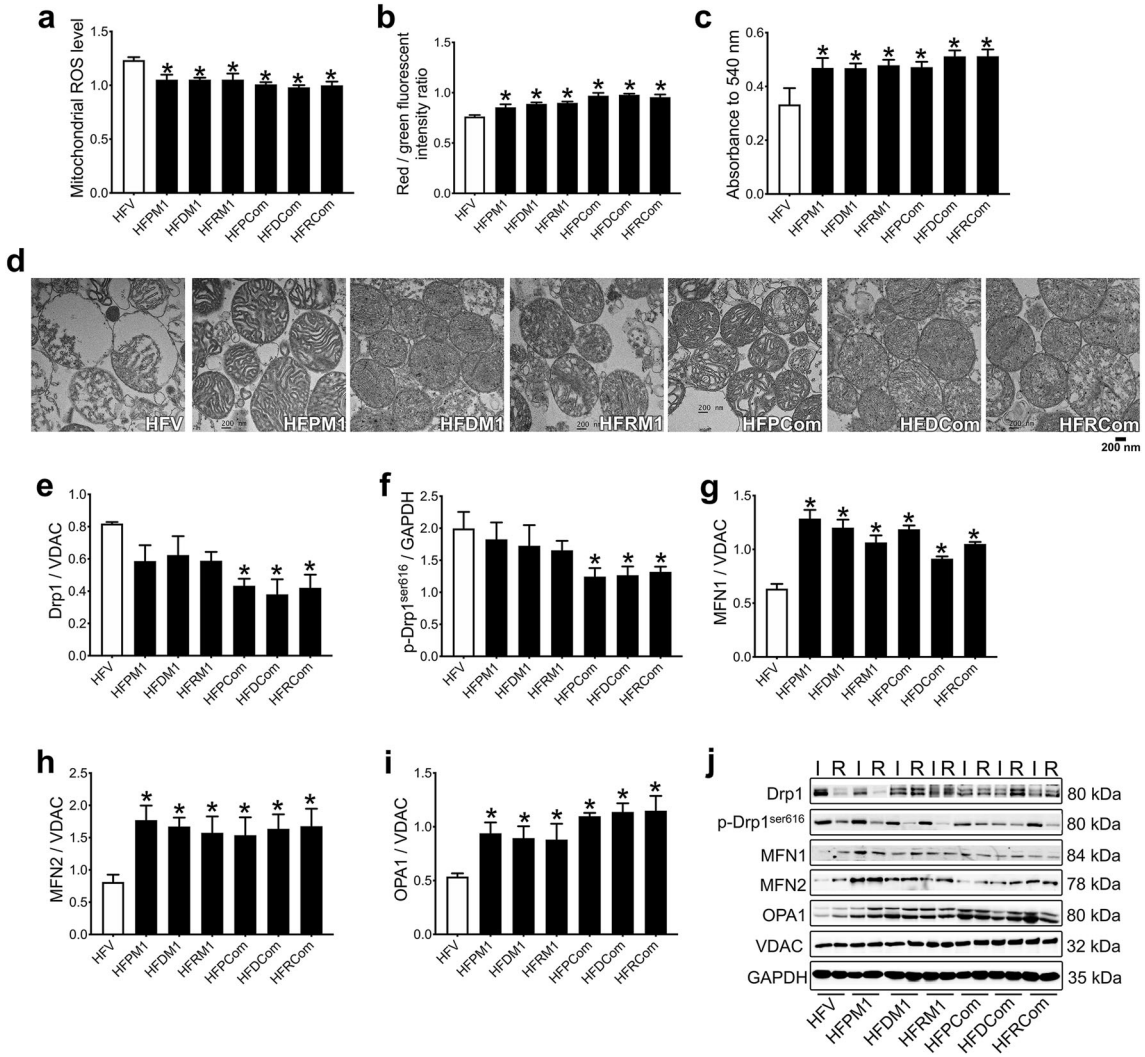

Fig. 4 The effects of acute M1 and combined treatment at different time points on cardiac mitochondrial function and dynamic protein expression in prediabetic rats with cardiac I/R injury. a Mitochondrial ROS production; **b** Mitochondrial membrane potential changes (red to green fluorescence intensity ratio); **c** Mitochondrial swelling (absorbance at 540 nm); **d** TEM representative images of cardiac mitochondria (scale bar = 200 nm); **e** Drp1 expression in mitochondria; **f** p-Drp1^{ser616} expression in the cytosol; **g** Mfn1 expression in mitochondria; **h** Mfn2 expression in mitochondria; **i** Opa1 expression in mitochondria; **j** Representative images of Western blotting bands in the ischemic area normalized with that in the remote area. $n = 5$ per group. *$P < 0.05$ vs HFV. Drp1 dynamin-related protein 1, GAPDH glyceraldehyde 3-phosphate dehydrogenase, HFDCom high-fat diet-fed rats with Mdivi-1 and M1 treatment during ischemia, HFDM1 high-fat diet-fed rats with M1 treatment during ischemia, HFPCom high-fat diet-fed rats with Mdivi-1 and M1 treatment preischemia, HFPM1 high-fat diet-fed rats with M1 treatment preischemia, HFRCom high-fat diet-fed rats with Mdivi-1 and M1 treatment at the onset of reperfusion, HFRM1 high-fat diet-fed rats with M1 treatment at the onset of reperfusion, HFV high-fat diet-fed rats with vehicle treatment, Mfn1 mitofusin 1, Mfn2 mitofusin 2, Opa1 optic atrophy 1, p-Drp1^{ser616} phosphorylated Drp1 at serine 616, ROS reactive oxygen species, TEM transmission electron microscopy, VDAC voltage-dependent anion channel.

when compared with their ischemic period. There was no significant difference in HR among all groups at any time point during cardiac I/R injury (Fig. 6a). The combined treatment did not show any greater efficacy than M1 treatment alone.

DISCUSSION

This study explores the therapeutic efficacy of a mitochondrial fusion promoter (M1) and the additional effects of a mitochondrial fission inhibitor (Mdivi-1) administered with M1 at different periods (before ischemia, during ischemia and at the onset of reperfusion) following cardiac I/R in rats with prediabetic conditions. Our novel finding is that single M1 therapy attenuated the impairment of mitochondrial dynamics and function in prediabetic I/R rats, leading to reductions in arrhythmias, myocardial cell death, infarct size, and cardiac dysfunction. In addition to M1 treatment alone, the combined therapy also provided a similar cardioprotective effect and did not provide any additional benefit in a rat model of prediabetes with I/R injury. Therefore, balancing the dynamic processes by promoting mitochondrial fusion in cardiac mitochondria may represent a promising novel therapy for prediabetic cardiac complications. A schematic diagram summarizing the effects of M1 given at different time points during cardiac I/R injury in prediabetic rats is shown in Fig. 7.

Excessive mitochondrial fission or fragmentation has been implicated in the pathogenesis of a variety of disorders, including cancer, neurodegenerative disease, obesity, and cardiovascular diseases [24, 40, 41]. Targeting mitochondrial fission via a Drp1 inhibitor (Mdivi-1) administered 15 min before the onset of

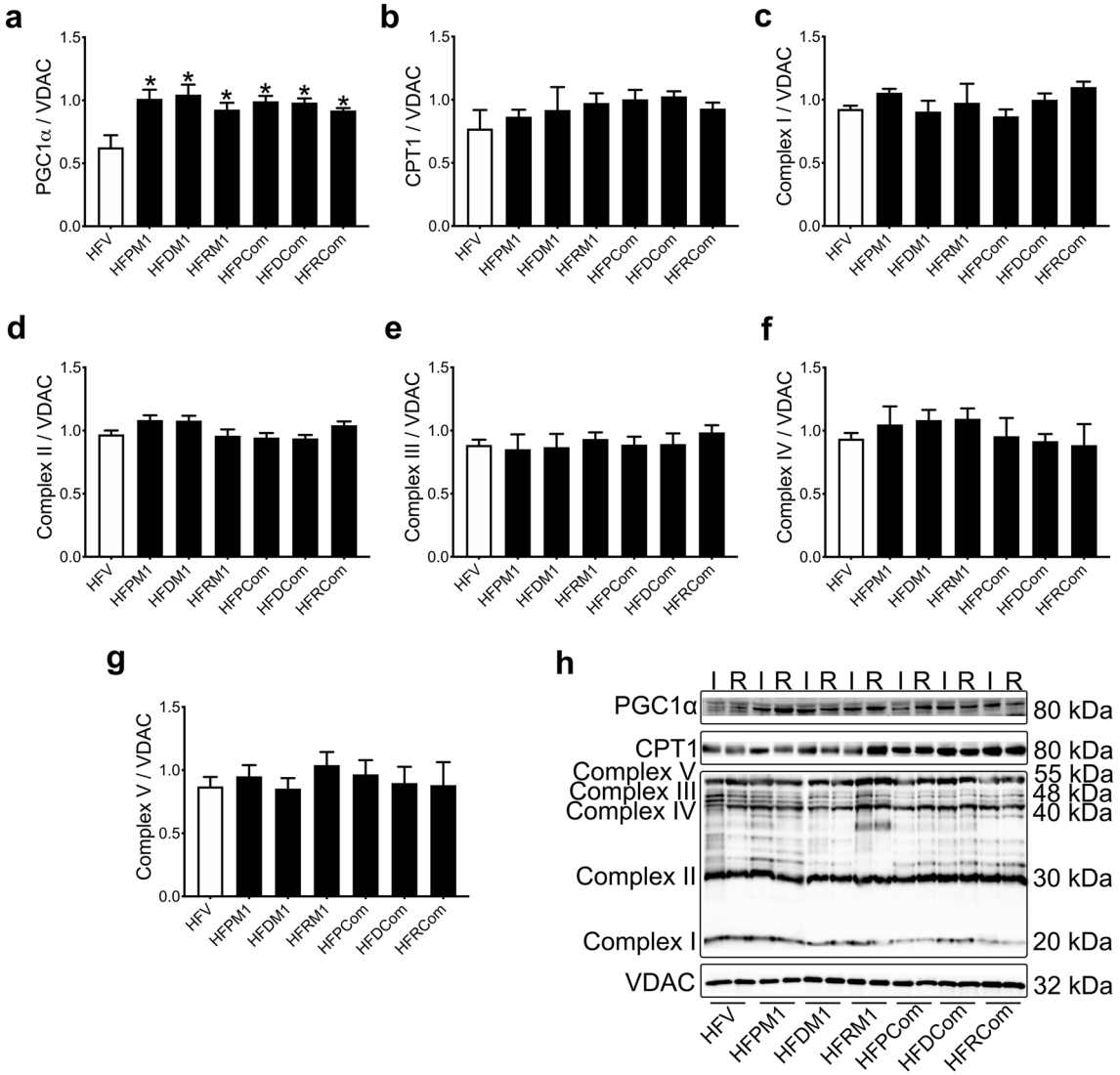

Fig. 5 The effects of acute M1 and combined treatment at different time points on cardiac mitochondrial biogenesis and mitochondrial respiratory complex expression of electron transport chain proteins in prediabetic rats with cardiac I/R injury. a PGC1-α expression in mitochondria; **b** CPT1 expression in mitochondria; **c** Complex I expression in mitochondria; **d** Complex II expression in mitochondria; **e** Complex III expression in mitochondria; **f** Complex IV expression in mitochondria; **g** Complex V expression in mitochondria; **h** Representative images of Western blotting bands in the ischemic area normalized with that in the remote area. $n = 5$ per group. *$P < 0.05$ vs HFV. CPT1 carnitine palmitoyltransferase I, HFDCom high-fat diet-fed rats with Mdivi-1 and M1 treatment during ischemia, HFDM1 high-fat diet-fed rats with M1 treatment during ischemia, HFPCom high-fat diet-fed rats with Mdivi-1 and M1 treatment preischemia, HFPM1 high-fat diet-fed rats with M1 treatment preischemia, HFRCom high-fat diet-fed rats with Mdivi-1 and M1 treatment at the onset of reperfusion, HFRM1 high-fat diet-fed rats with M1 treatment at the onset of reperfusion, HFV high-fat diet-fed rats with vehicle treatment, PGC1-α peroxisome proliferator-activated receptor gamma coactivator 1-alpha, VDAC voltage-dependent anion channel.

reperfusion prevented mitochondrial fission and reduced myocardial I/R injury in diabetic mice [42]. Since myocardial ischemia is an acute and unpredictable event, the therapeutic interventions given at the time of ischemia or reperfusion that reduce this cardiac injury would be more meaningful in mimicking clinical scenarios. Therefore, these findings suggested that inhibition of mitochondrial fission could be a promising intervention with the potential to afford cardioprotection in clinical settings of acute myocardial infarction in cases of prediabetes. In addition to excessive fission, impaired mitochondrial fusion, as indicated by a reduction in Mfn1/2 and Opa1, was also linked to I/R injury with obesity [31, 34, 43, 44]. In this study, we further investigated the beneficial effects of promoting fusion by using the mitochondrial fusion promoter M1 (M1) in a scenario of cardiac I/R in prediabetic conditions. We also investigated whether adding a fission inhibitor (Mdivi-1) to M1 treatment would provide more cardioprotection under these conditions.

In this study, a single dose of M1 was given after 15 min of myocardial ischemia and at the onset of reperfusion to promote mitochondrial dynamics regulation and mitochondrial function. Following this, myocardial infarction and LV dysfunction were alleviated as a consequence of the improvement in mitochondrial dynamics and function. Therefore, this study not only found that promotion of fusion can restore mitochondrial dynamics balance and its function, but it also revealed how the cardiac injury was reduced and how accompanying functional outcomes were improved in the prediabetic-I/R condition. It was found that the combination of promoting fusion by M1 and inhibiting fission by Mdivi-1 did not enhance the level of efficacy when compared to the single M1 treatment, suggesting that the enhanced

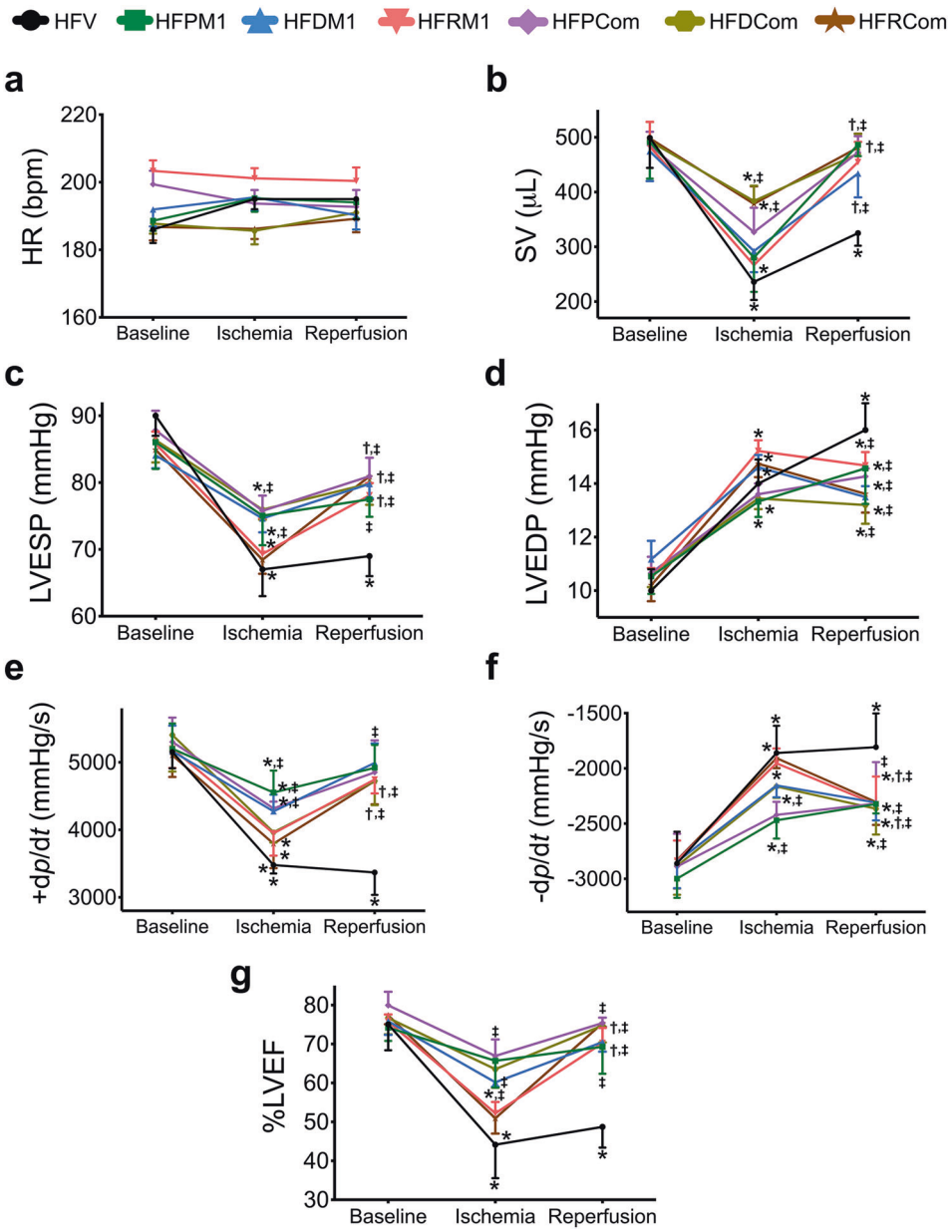

Fig. 6 The effects of acute M1 and combined treatment at different time points on LV function in prediabetic rats with cardiac I/R injury. **a** HR; **b** SV; **c** LVESP; LVEDP; **e** +d*p*/d*t*; **f** -d*p*/d*t*; **g** %LVEF. $n = 5$ per group. $^{*}P < 0.05$ compared with the baseline within a group; $^{\dagger}P < 0.05$ compared with ischemia within a group; $^{\ddagger}P < 0.05$ compared with the control group at that time period. +d*p*/d*t* maximum rate of rise of left ventricular pressure, -d*p*/d*t* minimum rate of rise of left ventricular pressure, HFDCom high-fat diet-fed rats with Mdivi-1 and M1 treatment during ischemia, HFDM1 high-fat diet-fed rats with M1 treatment during ischemia, HFPCom high-fat diet-fed rats with Mdivi-1 and M1 treatment preischemia, HFPM1 high-fat diet-fed rats with M1 treatment preischemia, HFRCom high-fat diet-fed rats with Mdivi-1 and M1 treatment at the onset of reperfusion, HFRM1 high-fat diet-fed rats with M1 treatment at the onset of reperfusion, HFV high-fat diet-fed rats with vehicle treatment, HR heart rate, LVEDP left ventricular end-diastolic pressure, LVEF left ventricular ejection fraction, LVESP left ventricular end-systolic pressure, SV stroke volume.

mitochondrial fusion strategy was sufficient to protect the heart against I/R injury under prediabetic conditions.

Our results showed that either differential temporal promotion of mitochondrial fusion by M1 or combined M1 with Mdivi-1 at the time points prior to myocardial ischemia, during ischemia, and upon the onset of reperfusion exerted similar levels of cardioprotective efficacy in a prediabetic rat model of cardiac I/R injury. Regarding the similar cardioprotective benefits of M1 and combined treatment at the three different time points following cardiac I/R injury, it has been reported that cardiac I/R injury is associated with cardiac mitochondrial damage and altered fission-fusion balance, leading to mitochondrial fragmentation and myocardial cell death [45]. During cardiac ischemia, an increase in oxidative stress, mitochondrial ROS production, and mitochondrial membrane depolarization aggravated mitochondrial dysfunction. However, during reperfusion, an increase in mitochondrial fission with impaired fusion will then be triggered to mediate mitochondrial fragmentation. These fragmented mitochondria are associated with apoptotic cell death and cardiac dysfunction following I/R injury [46]. In this study, administering M1 and combined treatment either during ischemia or at the onset of reperfusion demonstrated similar efficacy on cardiac

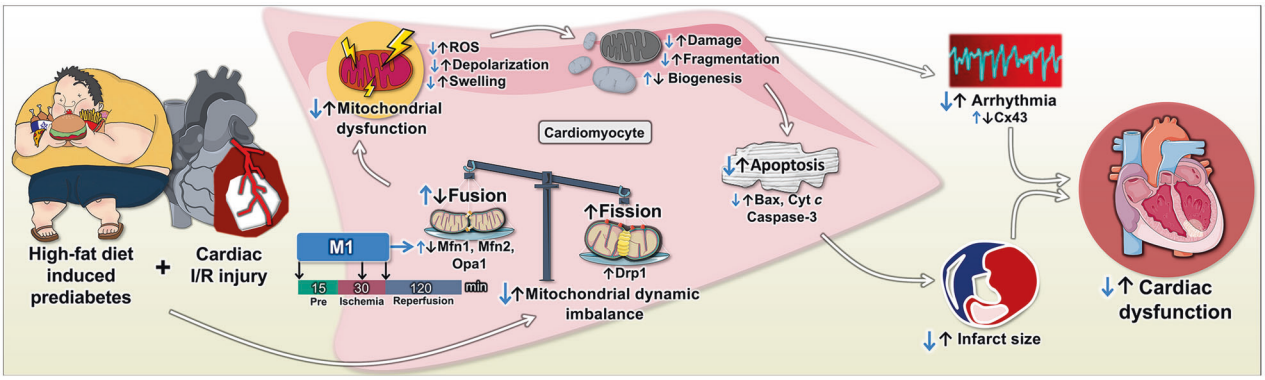

Fig. 7 Schematic diagram summarizing the effects of acute M1 treatment administered at different time points on mitochondrial dynamics, mitochondrial function, apoptosis, infarction, arrhythmia, and cardiac function in prediabetic rats with cardiac I/R injury. Differential temporal promotion of mitochondrial fusion via M1 alleviated the dynamic imbalance of cardiac mitochondria and reduced mitochondrial dysfunction, leading to decreased cardiac arrhythmia and ameliorated cardiac dysfunction. In addition, an improvement in mitochondrial function also mitigated mitochondrial damage and fragmentation, resulting in a decrease in myocardial apoptosis and infarct size and ultimately improved cardiac function.

function. This possibility of similar cardioprotective effects could be due to the ability of M1 and Mdivi-1 to prevent mitochondrial fragmentation. In our previous studies in lean rats with cardiac I/R injury, we showed that either M1 or Mdivi-1 treatment at all time points effectively restored the expression of mitochondrial fusion-related proteins, including Mfn1/2 and Opa1, compared with sham-operated lean rats under I/R conditions [18, 27]. These findings indicated that M1 and combined treatment at three different I/R time points effectively promoted mitochondrial fusion with the same maximum efficacy. In this study, in prediabetic rats, we also observed a similar promotion of Mfn1/2 and Opa1; thus, mitochondrial dysmorphism and mitochondrial dysfunction might also be attenuated to a comparable extent.

It has been well documented that cardiac I/R induces excessive mitochondrial fission-mediated fragmentation, which culminates in myocardial cell death and cardiac dysfunction [45]. We demonstrated in previous studies that Mdivi-1, a fission inhibitor, effectively suppressed both p-Drp1^{ser616} and total Drp1 expression, leading to reduced myocardial cell death and attenuated cardiac dysfunction in an I/R injury model [18, 32]. We also reported that M1, the fusion promoter, possessed cardioprotective effects against I/R injury, resulting in improvements in functional parameters similar to those resulting from Mdivi-1 treatment [27]. Since the primary effect of M1 is to shift the balance of mitochondrial dynamics toward fusion, it is reasonable to propose that mitochondrial fission-induced fragmentation may serve as a downstream common pathway where the effects of both therapeutic strategies (fusion promotion and fission inhibition) eventually converge. For this reason, either M1 alone or the combined treatment could exert mito- and cardioprotection through this downstream common pathway, and the synergistic effect would be indemonstrable once the pathway has already been fully activated. There is some evidence to suggest that HFD-induced diabetes and metabolic syndrome result in decreased mitochondrial density and reduced production of mitochondrial proteins due to mitochondrial DNA mutations [47]. In addition, mitochondria in ischemic cardiac myocytes appeared less dense and smaller (29% reduction in size) than those in the sham group [48]. Therefore, modulating mitochondrial dynamics via M1 or Mdivi-1 might have an impact on mitochondrial volume and number in cardiac I/R injury with prediabetes. Future studies are needed to investigate these issues to support the results of mitochondrial function and their dynamic protein expression.

Mitochondrial dysfunction and mitochondrial dynamics imbalance in cardiac I/R injury are the major focus of the present study. However, mitophagy, which is generally a downstream process for the clearance of dysfunctional and fragmented mitochondria, has been shown to be reduced by cardiac I/R injury, eventually leading to cardiomyocyte apoptosis [49, 50]. This finding has led to the speculation that potentiating mitophagy may mitigate I/R injury-induced cardiac cell death, which has been supported by several studies [51, 52]. Unfortunately, the appropriate direction for pharmacological modulation of mitophagy remains debatable since reports on the beneficial effects of mitophagy inhibition also exist [53–55]. Given that mitophagy generally acts downstream of mitochondrial dynamics control, the appropriate shift in mitophagic flux may also contribute to the benefits of M1 and M1 + Mdivi-1 treatment. Therefore, it would be useful to determine how (in which direction and to what extent) these mitochondrial modulators affect mitophagy in future studies.

Mitochondrial fusion protects against apoptosis, while mitochondrial fission is associated with most forms of cell death [56]. Several studies of multiple apoptotic systems have revealed causal links between mitochondrial dynamics and the induction of cell death [57, 58]. During apoptosis, mitochondria become fragmented, a process dependent on the translocation of Drp1 from the cytosol to mitochondria and the degradation of fusion proteins. We have previously shown that an increase in Drp1-induced excessive fission and loss of fusion were accompanied by the enhancement of myocardial apoptosis in prediabetic animals [33]. In this study, the promotion of fusion significantly suppressed myocardial apoptosis, as evidenced by decreased protein-related apoptosis (Bax, Cyt *c*, cleaved caspase-3) and TUNEL-positive cells at all treated time periods following cardiac I/R injury in prediabetic models. Generally, caspases also play a critical role in cardiac cell death in I/R injury [59]. Prolonged periods of myocardial ischemia are related to an increase in the rate of necrosis, whereas reperfusion paradoxically leads to an enhancement in apoptosis. There is more supportive evidence for ischemia-related apoptosis, as mitochondrial dysfunction has been demonstrated with leakage of Cyt *c* and caspase activation. Previous studies using nonspecific inhibition of caspases have been shown to be therapeutically beneficial in myocardial I/R-induced damage [60]. Moreover, caspase inhibition during early reperfusion also protected the myocardium against lethal reperfusion injury [61]. Our data suggested that impaired mitochondrial fusion plays a pivotal role in myocardial apoptosis, a major form of cell death following prediabetic I/R injury, because the combination therapy, adding Mdivi-1 to M1, did not result in any benefit.

With regard to the potential benefits of M1 treatment, we also found an upregulation of the expression of p-Cx43^{ser368}, a

Table 2. A summary of the effects of M1 and combined treatment on cardiac mitochondrial function and LV function given at different time-points during cardiac I/R injury in pre-diabetic rats.

Parameters	HFV	HFPM1	HFDM1	HFRM1	HFPCom	HFDCom	HFRCom
Infarct size	↔	↓	↓	↓	↓	↓	↓
Mortality rate	↔	↓	↓	↓	↓	↓	↓
Arrhythmia score	↔	↓	↓	↓	↓	↓	↓
Phosphorylated connexin 43 (Ser368)	↔	↑	↑	↑	↑	↑	↑
Cardiac apoptosis	↔	↓	↓	↓	↓	↓	↓
Mitochondrial function	↔	↑	↑	↑	↑	↑	↑
Mitochondrial fission	↔	↓	↓	↓	↓	↓	↓
Mitochondrial fusion	↔	↑	↑	↑	↑	↑	↑
Mitochondrial biogenesis	↔	↑	↑	↑	↑	↑	↑
Mitochondrial oxidative metabolism	↔	↔	↔	↔	↔	↔	↔
Mitochondrial oxidative phosphorylation	↔	↔	↔	↔	↔	↔	↔
Cardiac function	↔	↑	↑	↑	↑	↑	↑

HFDCom high-fat-diet fed rats with Mdivi-1 and M1 treatment during ischemia, *HFDM1* high-fat-diet fed rats with M1 treatment during ischemia, *HFPCom* high-fat-diet fed rats with Mdivi-1 and M1 treatment preischemia, *HFPM1* high-fat-diet fed rats with M1 treatment preischemia, *HFRCom* high-fat-diet fed rats with Mdivi-1 and M1 treatment at the onset of reperfusion, *HFRM1* high-fat-diet fed rats with M1 treatment at the onset of reperfusion, *HFV* high-fat-diet fed rats with vehicle treatment.

reduction in myocardial infarct size, and an improvement in cardiac function in both the M1 and combined treatment groups. All these benefits were similar following both types of treatment; therefore, these findings indicate that M1 was sufficient to provide cardioprotection since adding Mdivi-1 to M1 did not enhance any of the aspects investigated. Cx43 is the major protein in cardiac ventricular gap junctions and is crucial for cell-to-cell communication and cardiac function [62]. Remodeling the cellular distribution in gap junctions formed mainly by Cx43 can be related to the increased incidence of cardiac arrhythmias [63]. In addition, the oscillation of the mitochondrial membrane by increasing mitochondrial depolarization could increase fatal cardiac arrhythmias following cardiac I/R injury by downregulating Cx43 [64, 65]. In addition to the antiarrhythmic effects of increasing p-Cx43, M1 was effective in the suppression of I/R-induced myocardial infarction and cardiac dysfunction in these prediabetic animals.

The left ventricular ejection fraction (LVEF) during the ischemic period in the HFPM1, HFDM1, HFPCom, and HFDCom groups was comparable to their LVEF at baseline. The plausible reasons for this counterintuitive finding are that (1) the peripheral zone of the ARR could be partially supplied by collateral microcirculation, which allowed the drugs (M1 and Mdivi-1) given during LAD occlusion to reach the cardiomyocytes in such areas; and (2) these accessible cardiomyocytes were salvaged by the drugs to a comparable degree in the pretreatment and treatment during ischemia groups, resulting in similarly preserved LVEF (stated another way, a similar proportion of cells at the ischemic core were nonsalvageable regardless of the timing of treatment). These explanations are supported by the fact that the infarct sizes in the pretreatment and treatment during ischemia groups were not different in the present study, as shown in Fig. 2a, b.

It has been demonstrated that coronary collateral arteries could connect a region supplied by one epicardial artery with that supplied by another [66]. Moreover, it was possible to identify a peri-infarct area of viable, albeit ischemic, myocardial tissue that could be salvaged by pharmacological treatment in the diabetic murine model of acute myocardial infarction [67, 68]. Intriguingly, a study in a swine model of cardiac I/R by Duran et al. [69] reported that the majority of myocytes in the infarct zone are necrotic or undergo apoptosis, while the border zone represents a mixed population of dying and surviving myocytes. Accordingly, the border zone serves as a promising therapeutic target for myocardial salvage [69]. In line with these data, M1 and Mdivi-1, given either before or during ischemia, might improve cardiac function by preventing the progression of the peri-infarct area that is pharmacologically accessible and salvageable. This hypothesis should be tested by a future study that specifically determines the effects of these mitochondrial dynamics modulators on mitochondrial morphology and function, cellular energetics, and activation of cell death pathways in the peri-infarct zone within the AAR. A summary of these findings is shown in Table 2.

In conclusion, differential temporal modulations of the promotion of mitochondrial fusion exerted a similar cardioprotective efficacy against prediabetic I/R injury through the rebalancing of mitochondrial dynamics, leading to the attenuation of mitochondrial dysfunction and arrhythmias, reduction in infarct size, and improvement in cardiac function.

ACKNOWLEDGEMENTS

This work was supported by the NSTDA Research Chair grant from the National Science and Technology Development Agency Thailand (NC); the Thailand Research Fund grants TRF-Royal Golden Jubilee Program [grant numbers PHD/0144/2558] (CM and NC); the Senior Research Scholar Grant from the National Research Council of Thailand (SCC); and the Chiang Mai University Center of Excellence Award (NC).

AUTHOR CONTRIBUTIONS

CM performed the experiments, analyzed the data, and wrote the manuscript. SP performed the experiments and analyzed data. SK and TJ performed the experiments. SCC designed the study, contributed to the discussion, and edited the manuscript. NC designed the study, analyzed the data, contributed to the discussion, and edited and finalized the manuscript.

ADDITIONAL INFORMATION

Competing interests: The authors declare no competing interests.

REFERENCES

1. De Lorenzo A, Gratteri S, Gualtieri P, Cammarano A, Bertucci P, Di Renzo L. Why primary obesity is a disease? J Transl Med. 2019;17:169.

2. Mongraw-Chaffin M, Foster MC, Anderson CAM, Burke GL, Haq N, Kalyani RR, et al. Metabolically healthy obesity, transition to metabolic syndrome, and cardiovascular risk. J Am Coll Cardiol. 2018;71:1857–65.
3. Kachur S, Lavie CJ, de Schutter A, Milani RV, Ventura HO. Obesity and cardiovascular diseases. Minerva Med. 2017;108:212–28.
4. Jahangir E, De Schutter A, Lavie CJ. The relationship between obesity and coronary artery disease. Transl Res. 2014;164:336–44.
5. Hausenloy DJ, Yellon DM. Myocardial ischemia-reperfusion injury: a neglected therapeutic target. J Clin Invest. 2013;123:92–100.
6. Hausenloy DJ, Botker HE, Engstrom T, Erlinge D, Heusch G, Ibanez B, et al. Targeting reperfusion injury in patients with st-segment elevation myocardial infarction: trials and tribulations. Eur Heart J. 2017;38:935–41.
7. Davidson SM, Ferdinandy P, Andreadou I, Botker HE, Heusch G, Ibanez B, et al. Multitarget strategies to reduce myocardial ischemia/reperfusion injury: jacc review topic of the week. J Am Coll Cardiol. 2019;73:89–99.
8. Hausenloy DJ, Barrabes JA, Botker HE, Davidson SM, Di Lisa F, Downey J, et al. Ischaemic conditioning and targeting reperfusion injury: a 30 year voyage of discovery. Basic Res Cardiol. 2016;111:70.
9. Feno S, Butera G, Vecellio Reane D, Rizzuto R, Raffaello A. Crosstalk between calcium and ros in pathophysiological conditions. Oxid Med Cell Longev. 2019;2019:9324018.
10. Ostadal B, Drahota Z, Houstek J, Milerova M, Ostadalova I, Hlavackova M, et al. Developmental and sex differences in cardiac tolerance to ischemia-reperfusion injury: the role of mitochondria (1). Can J Physiol Pharmacol. 2019;97:808–14.
11. Manning AS, Hearse DJ. Reperfusion-induced arrhythmias: mechanisms and prevention. J Mol Cell Cardiol. 1984;16:497–518.
12. Hearse DJ, Tosaki A. Free radicals and reperfusion-induced arrhythmias: protection by spin trap agent pbn in the rat heart. Circ Res. 1987;60:375–83.
13. Tosaki A. Arrhythmogenopharmacotherapy. Front Pharmacol. 2020;11:616.
14. Zhou T, Prather ER, Garrison DE, Zuo L. Interplay between ROS and antioxidants during ischemia-reperfusion injuries in cardiac and skeletal muscle. Int J Mol Sci. 2018;19:417.
15. Bertero E, Maack C. Calcium signaling and reactive oxygen species in mitochondria. Circ Res. 2018;122:1460–78.
16. Koncsos G, Varga ZV, Baranyai T, Boengler K, Rohrbach S, Li L, et al. Diastolic dysfunction in prediabetic male rats: role of mitochondrial oxidative stress. Am J Physiol Heart Circ Physiol. 2016;311:H927–43.
17. Ong SB, Subrayan S, Lim SY, Yellon DM, Davidson SM, Hausenloy DJ. Inhibiting mitochondrial fission protects the heart against ischemia/reperfusion injury. Circulation. 2010;121:2012–22.
18. Maneechote C, Palee S, Kerdphoo S, Jaiwongkam T, Chattipakorn SC, Chattipakorn N. Differential temporal inhibition of mitochondrial fission by mdivi-1 exerts effective cardioprotection in cardiac ischemia/reperfusion injury. Clin Sci. 2018;132:1669–83.
19. Dong Y, Undyala VVR, Przyklenk K. Inhibition of mitochondrial fission as a molecular target for cardioprotection: critical importance of the timing of treatment. Basic Res Cardiol. 2016;111:59.
20. Ferree A, Shirihai O. Mitochondrial dynamics: the intersection of form and function. Adv Exp Med Biol. 2012;748:13–40.
21. Whitley BN, Engelhart EA, Hoppins S. Mitochondrial dynamics and their potential as a therapeutic target. Mitochondrion. 2019;49:269–83.
22. Chan DC. Mitochondrial dynamics and its involvement in disease. Annu Rev Pathol. 2019;15:235–59.
23. Kornfeld OS, Qvit N, Haileselassie B, Shamloo M, Bernardi P, Mochly-Rosen D. Interaction of mitochondrial fission factor with dynamin related protein 1 governs physiological mitochondrial function in vivo. Sci Rep. 2018;8:14034.
24. Maneechote C, Palee S, Chattipakorn SC, Chattipakorn N. Roles of mitochondrial dynamics modulators in cardiac ischaemia/reperfusion injury. J Cell Mol Med. 2017;21:2643–53.
25. Maneechote C, Palee S, Apaijai N, Kerdphoo S, Jaiwongkam T, Chattipakorn SC, et al. Mitochondrial dynamic modulation exerts cardiometabolic protection in obese insulin-resistant rats. Clin Sci. 2019;133:2431–47.
26. Pei H, Yang Y, Zhao H, Li X, Yang D, Li D, et al. The role of mitochondrial functional proteins in ROS production in ischemic heart diseases. Oxid Med Cell Longev. 2016;2016:5470457.
27. Maneechote C, Palee S, Kerdphoo S, Jaiwongkam T, Chattipakorn SC, Chattipakorn N. Balancing mitochondrial dynamics via increasing mitochondrial fusion attenuates infarct size and left ventricular dysfunction in rats with cardiac ischemia/reperfusion injury. Clin Sci. 2019;133:497–513.
28. Sharp WW, Fang YH, Han M, Zhang HJ, Hong Z, Banathy A, et al. Dynamin-related protein 1 (Drp1)-mediated diastolic dysfunction in myocardial ischemia-reperfusion injury: therapeutic benefits of drp1 inhibition to reduce mitochondrial fission. FASEB J. 2014;28:316–26.
29. Givvimani S, Pushpakumar SB, Metreveli N, Veeranki S, Kundu S, Tyagi SC. Role of mitochondrial fission and fusion in cardiomyocyte contractility. Int J Cardiol. 2015;187:325–33.
30. Jheng HF, Tsai PJ, Guo SM, Kuo LH, Chang CS, Su IJ, et al. Mitochondrial fission contributes to mitochondrial dysfunction and insulin resistance in skeletal muscle. Mol Cell Biol. 2012;32:309–19.
31. Dai W, Jiang L. Dysregulated mitochondrial dynamics and metabolism in obesity, diabetes, and cancer. Front Endocrinol. 2019;10:570.
32. Maneechote C, Palee S, Kerdphoo S, Jaiwongkam T, Chattipakorn SC, Chattipakorn N. Pharmacological inhibition of mitochondrial fission attenuates cardiac ischemia-reperfusion injury in pre-diabetic rats. Biochem Pharmacol. 2020;182:114295.
33. Maneechote C, Palee S, Apaijai N, Kerdphoo S, Jaiwongkam T, Chattipakorn SC, et al. Mitochondrial dynamic modulation exerts cardiometabolic protection in obese insulin-resistant rats. Clin Sci. 2019;133:2431–47.
34. Ding M, Liu C, Shi R, Yu M, Zeng K, Kang J, et al. Mitochondrial fusion promoter restores mitochondrial dynamics balance and ameliorates diabetic cardiomyopathy in an optic atrophy 1-dependent way. Acta Physiol. 2020;229:e13428.
35. Percie du Sert N, Hurst V, Ahluwalia A, Alam S, Avey MT, Baker M, et al. The arrive guidelines 2.0: updated guidelines for reporting animal research. PLoS Biol. 2020;18:e3000410.
36. National Research Council (US) Committee for the Update of the Guide for the Care and Use of Laboratory Animals. Guide for the care and use of laboratory animals. Washington (DC): National Academies Press (US);2011.
37. Pratchayasakul W, Kerdphoo S, Petsophonsakul P, Pongchaidecha A, Chattipakorn N, Chattipakorn SC. Effects of high-fat diet on insulin receptor function in rat hippocampus and the level of neuronal corticosterone. Life Sci. 2011;88:619–27.
38. Thummasorn S, Kumfu S, Chattipakorn S, Chattipakorn N. Granulocyte-colony stimulating factor attenuates mitochondrial dysfunction induced by oxidative stress in cardiac mitochondria. Mitochondrion. 2011;11:457–66.
39. Apaijai N, Chinda K, Palee S, Chattipakorn S, Chattipakorn N. Combined vildagliptin and metformin exert better cardioprotection than monotherapy against ischemia-reperfusion injury in obese-insulin resistant rats. PLoS One. 2014;9:e102374.
40. Serasinghe MN, Chipuk JE. Mitochondrial fission in human diseases. Handb Exp Pharmacol. 2017;240:159–88.
41. Roy S, Kim D, Sankaramoorthy A. Mitochondrial structural changes in the pathogenesis of diabetic retinopathy. J Clin Med. 2019;8:1363.
42. Ding M, Dong Q, Liu Z, Liu Z, Qu Y, Li X, et al. Inhibition of dynamin-related protein 1 protects against myocardial ischemia-reperfusion injury in diabetic mice. Cardiovasc Diabetol. 2017;16:19.
43. Lopez-Lluch G. Mitochondrial activity and dynamics changes regarding metabolism in ageing and obesity. Mech Ageing Dev. 2017;162:108–21.
44. Heo JW, No MH, Park DH, Kang JH, Seo DY, Han J, et al. Effects of exercise on obesity-induced mitochondrial dysfunction in skeletal muscle. Korean J Physiol Pharmacol. 2017;21:567–77.
45. Mui D, Zhang Y. Mitochondrial scenario: Roles of mitochondrial dynamics in acute myocardial ischemia/reperfusion injury. J Recept Signal Transduct Res. 2021;41:1–5.
46. Kulek AR, Anzell A, Wider JM, Sanderson TH, Przyklenk K. Mitochondrial quality control: role in cardiac models of lethal ischemia-reperfusion injury. Cells. 2020;9:214.
47. Siasos G, Tsigkou V, Kosmopoulos M, Theodosiadis D, Simantiris S, Tagkou NM, et al. Mitochondria and cardiovascular diseases-from pathophysiology to treatment. Ann Transl Med. 2018;6:256.
48. Galan DT, Bito V, Claus P, Holemans P, Abi-Char J, Nagaraju CK, et al. Reduced mitochondrial respiration in the ischemic as well as in the remote nonischemic region in postmyocardial infarction remodeling. Am J Physiol Heart Circ Physiol. 2016;311:H1075–90.
49. Fakhry M, Skafi N, Fayyad-Kazan M, Kobeissy F, Hamade E, Mebarek S, et al. Characterization and assessment of potential micrornas involved in phosphate-induced aortic calcification. J Cell Physiol. 2018;233:4056–67.
50. Lesnefsky EJ, Chen Q, Tandler B, Hoppel CL. Mitochondrial dysfunction and myocardial ischemia-reperfusion: implications for novel therapies. Annu Rev Pharmacol Toxicol. 2017;57:535–65.
51. Zhang W, Siraj S, Zhang R, Chen Q. Mitophagy receptor fundc1 regulates mitochondrial homeostasis and protects the heart from I/R injury. Autophagy. 2017;13:1080–1.
52. Liu XW, Lu MK, Zhong HT, Wang LH, Fu YP. Panax notoginseng saponins attenuate myocardial ischemia-reperfusion injury through the hif-1α/bnip3 pathway of autophagy. J Cardiovasc Pharmacol. 2019;73:92–9.
53. Moyzis AG, Sadoshima J, Gustafsson ÅB. Mending a broken heart: the role of mitophagy in cardioprotection. Am J Physiol Heart Circ Physiol. 2015;308:H183–92.
54. Kubli DA, Gustafsson ÅB. Mitochondria and mitophagy: the yin and yang of cell death control. Circ Res. 2012;111:1208–21.

55. Feng Y, Madungwe NB, da Cruz Junho CV, Bopassa JC. Activation of g protein-coupled oestrogen receptor 1 at the onset of reperfusion protects the myocardium against ischemia/reperfusion injury by reducing mitochondrial dysfunction and mitophagy. Br J Pharmacol. 2017;174:4329–44.
56. Suen DF, Norris KL, Youle RJ. Mitochondrial dynamics and apoptosis. Genes Dev. 2008;22:1577–90.
57. Jahani-Asl A, Germain M, Slack RS. Mitochondria: joining forces to thwart cell death. Biochim Biophys Acta. 2010;1802:162–6.
58. Hoppins S, Nunnari J. Cell biology. Mitochondrial dynamics and apoptosis-the ER connection. Science. 2012;337:1052–4.
59. Eefting F, Rensing B, Wigman J, Pannekoek WJ, Liu WM, Cramer MJ, et al. Role of apoptosis in reperfusion injury. Cardiovasc Res. 2004;61:414–26.
60. Kovacs P, Bak I, Szendrei L, Vecsernyes M, Varga E, Blasig IE, et al. Non-specific caspase inhibition reduces infarct size and improves post-ischaemic recovery in isolated ischaemic/reperfused rat hearts. Naunyn Schmiedebergs Arch Pharmacol. 2001;364:501–7.
61. Mocanu MM, Baxter GF, Yellon DM. Caspase inhibition and limitation of myocardial infarct size: protection against lethal reperfusion injury. Br J Pharmacol. 2000;130:197–200.
62. Xia Y, Gong KZ, Xu M, Zhang YY, Guo JH, Song Y, et al. Regulation of gap-junction protein connexin 43 by beta-adrenergic receptor stimulation in rat cardiomyocytes. Acta Pharmacol Sin. 2009;30:928–34.
63. Kohutova J, Elsnicova B, Holzerova K, Neckar J, Sebesta O, Jezkova J, et al. Anti-arrhythmic cardiac phenotype elicited by chronic intermittent hypoxia is associated with alterations in connexin-43 expression, phosphorylation, and distribution. Front Endocrinol. 2018;9:789.
64. Lampe PD, TenBroek EM, Burt JM, Kurata WE, Johnson RG, Lau AF. Phosphorylation of connexin43 on serine368 by protein kinase c regulates gap junctional communication. J Cell Biol. 2000;149:1503–12.
65. Yang L, Korge P, Weiss JN, Qu Z. Mitochondrial oscillations and waves in cardiac myocytes: insights from computational models. Biophys J. 2010;98:1428–38.
66. Meier P, Schirmer SH, Lansky AJ, Timmis A, Pitt B, Seiler C. The collateral circulation of the heart. BMC Med. 2013;11:143.
67. Toma I, Kim PJ, Dash R, McConnell MV, Nishimura D, Harnish P, et al. Telmisartan in the diabetic murine model of acute myocardial infarction: dual contrast manganese-enhanced and delayed enhancement mri evaluation of the peri-infarct region. Cardiovasc Diabetol. 2016;15:24.
68. Friedrich MG, Abdel-Aty H, Taylor A, Schulz-Menger J, Messroghli D, Dietz R. The salvaged area at risk in reperfused acute myocardial infarction as visualized by cardiovascular magnetic resonance. J Am Coll Cardiol. 2008;51:1581–7.
69. Duran JM, Taghavi S, Berretta RM, Makarewich CA, Sharp Iii T, Starosta T, et al. A characterization and targeting of the infarct border zone in a swine model of myocardial infarction. Clin Transl Sci. 2012;5:416–21.